ELSEVIER

Journal of Crystal Growth 243 (2002) 503–516

JOURNAL OF CRYSTAL GROWTH

www.elsevier.com/locate/jcrysgro

Effects of ferrocyanide ions on NaCl crystallization in porous stone

Carlos Rodriguez-Navarro[a,*], Lucia Linares-Fernandez[a], Eric Doehne[b], Eduardo Sebastian[a]

[a] *Departamento de Mineralogía y Petrología, Universidad de Granada, Fuentenueva s/n, 18002 Granada, Spain*
[b] *The Getty Conservation Institute, 1200 Getty Center Drive 700, Los Angeles, CA 90409, USA*

Received 22 May 2002; accepted 4 June 2002
Communicated by R. Kern

Abstract

The effects of $[Fe(CN)_6]^{4-}$ ions on the crystallization of NaCl in aqueous solution has been studied, particularly in the situation where the saline fluid percolates through and evaporates from a saturated porous body (i.e., an ornamental porous limestone). In concentrations ranging from 2.48×10^{-4} up to $2.85\,10^{-3}$ M the additive was able to increase the solution critical supersaturation (up to 8%) resulting in a significant crystallization inhibition effect, which promoted efflorescence growth on the porous stone surface as opposed to subflorescence growth. The former induced no damage to the stone support while the latter always resulted in crystallization pressure development inside the pores, causing granular disintegration—a process also known as "salt weathering". Significant changes in NaCl crystal growth morphology (from {1 0 0} towards {1 1 0}, {1 1 1} and {2 1 0} forms) were observed in the presence of ferrocyanide ions, which also promoted the growth of dendrites with their main growth axis parallel to ⟨1 1 1⟩, and branched along ⟨1 0 0⟩, at the highest supersaturation. The possible inhibiting mechanism of ferrocyanide on NaCl crystallization and growth is discussed based on the evolution of NaCl growth morphologies, and some practical applications of ferrocyanides to prevent salt damage and enhance desalination in ornamental stones are outlined.

PACS: 81.10.Aj; 61.50.Ah; 81.10.Dn; 83.80.Nb; 81.05.Rm

Keywords: A1. Crystal morphology; A1. Nucleation; A1. X-ray diffraction; A2. Growth from solutions; B1. Sodium chloride

1. Introduction

The important effects of some foreign ions and molecules (additives) on the growth of salt crystals in aqueous solutions have been known for centuries [1,2]. One of the earliest known examples is urea which induced habit changes (from cube to octahedron) in NaCl crystals [3]. Additives, also known as impurities, admixtures, inhibitors or poisons [4], are believed to act in two principal ways: (a) as crystallization inhibitors, preventing or delaying the formation of stable nuclei (i.e.,

*Corresponding author. Tel.: +34-958-243-340; fax: +34-958-243-368.
E-mail address: carlosrn@ugr.es (C. Rodriguez-Navarro).

0022-0248/02/$ - see front matter © 2002 Published by Elsevier Science B.V.
PII: S0022-0248(02)01499-9

with radius $\geqslant$ the critical radius), although in some instances additives can act as nucleation promoters [5]; and (b) as habit modifiers, by adsorption onto specific faces of a growing crystal, thus decreasing (or increasing) their growth rate. The literature on the topic is very extensive: see [1,6] and [7–11] for an early and more recent overviews, respectively.

Examples of well-known crystallization inhibitors and habit modifiers with extended technological and industrial uses are the families of polyphosphates and phosphates [12–18], carboxylates [19–21], polyacrylic acid derivatives [22] and benzotriazoles [23]. These additives are widely used as scale-inhibitors to prevent undesired effects associated with sparingly soluble salts (mainly sulfates and carbonates) precipitating in oil-extraction pipelines [24], industrial boilers, heat-exchangers, house-appliances or water pipes [18,23], mining and mineral processing [17], and desalination plants [15]. They are also used to delay cement [14] or gypsum plaster setting [21]. Despite the widespread use of crystallization inhibitors their action on nucleation and crystal growth is not yet fully understood.

Crystallization inhibitors have recently been tested as a new mean of preventing salt crystallization damage to porous ornamental stones [25]. Salt crystallization is an effective damage mechanism to construction materials and, particularly, to porous stones. This is due to the disruptive pressure exerted by a salt when it grows in a confined space, i.e., a pore [26–31]. The crystallization pressure [32] exerted by a salt toward the pore-wall is in many instances enough to overcome the tensile strength of most stones [32,33], which may lead to their crumbling or even total disintegration. Salt weathering is now recognized as a major construction and engineering hazard [34], being one of the most damaging weathering processes affecting the sculptural and architectural heritage [28].

Rodriguez-Navarro and co-workers [25] observed that sodium dodecyl sulfate (SDS) in saline solutions acted as a crystallization inhibitor, promoting the formation of sodium sulfate decahydrate crystals (mirabilite) on the surface of a porous limestone as efflorescence, rather than as harmful subflorescence. The latter occurs deep in the stone pores, and often results in significant damage [35,36]. By this mechanism, the surfactant was able to prevent/minimize salt damage. More recently, Selwitz and Doehne [37] continued this work using other crystallization inhibitors to prevent salt damage to porous stones. They found that while the tested surfactants/crystallization inhibitors showed some effectiveness against sodium sulfate crystallization damage, they did not show any significant amelioration effect in the presence of other common salts such as sodium chloride. The latter is one of the most abundant and ubiquitous salts found in weathered rocks and construction materials (e.g., stones and concrete) in a range of environments: from hot [38] and cold arid regions [39] to humid coastal areas [26]. Considering the reportedly strong inhibiting effects of ferrocyanide ions (FC) on NaCl crystallization [40–45], Selwitz and Doehne [37] postulated that they could act against NaCl as the surfactants described in [25] did against sodium sulfate crystallization damage to ornamental porous stones. Positive results on the potential use of FC to avoid salt crystallization damage due to NaCl subflorescence growth in porous stones have been reported using concentrations as low as 0.1 wt% [37]. Nevertheless, little is known about the effects of FC to the saline solution percolating and crystallizing in a porous media following evaporation (e.g., changes in evaporation rate, solution surface properties such as surface tension or contact angle, and critical supersaturation). FC have been known for decades as important NaCl crystallization inhibitors and effective habit modifiers, finding extensive use as anti-caking agents for road deicing salts [43,46,47] or as additives for the food-industry [48]. However, it is not fully understood if they act solely as nucleation inhibitors, therefore inducing morphology changes due to a general modification in the growth mechanisms at high supersaturation, or if they act as growth inhibitors, changing the halite crystals habit through preferential adsorption on specific faces; or if they act in both ways. A detailed study of halite growth morphologies as well as FC's inhibiting effects (i.e., level of

supersaturation reached before crystallization) could help resolve these questions.

Here we present the results of a systematic study of the effects of Na and K ferrocyanides (i.e., the so-called yellow Prussiates) on NaCl aqueous solution transport, evaporation and crystallization within a porous ornamental stone (i.e., limestone). These results allow a better understanding of the mechanisms of FC interaction on NaCl crystallization and growth. Also, the influence of FC on saline solution migration and evaporation within a porous media, as well as on NaCl far-from-equilibrium habit development, has been studied. Ultimately, this information may aid the development of new methods to preserve ornamental stones affected by NaCl crystallization damage, as well as better understanding the damage process.

2. Materials and methods

A stock NaCl saturated solution was prepared from crystalline solid (Panreac, analytical grade) using deionized water. The saturated solution was decanted to eliminate any undissolved NaCl crystal. Reagent grade (Sigma-Aldrich) sodium ferrocyanide ($Na_4Fe(CN)_6 \cdot 10H_2O$) or potassium ferrocyanide ($K_4Fe(CN)_6 \cdot 3H_2O$) were added to the NaCl saturated solution in concentrations ranging from 0.01% to 0.1% w/w. (i.e., 2.85×10^{-4} up to 2.85×10^{-3} M $K_4Fe(CN)_6 \cdot 3H_2O$, and 2.48×10^{-4} up to 2.48×10^{-3} M $Na_4Fe(CN)_6 \cdot 10H_2O$).

The solutions (with and without additive) were used for salt crystallization tests which were carried out in a room with controlled environment (20 ± 1°C, and 45 ± 5% relative humidity): (a) in a first run the solutions were let to evaporate in open glass beakers; and (b) in a second set of crystallization experiments the solutions were let to flow through, evaporate and crystallize in a porous stone (Fig. 1). The selected stone was a biomicritic limestone (calcarenite) from Granada (Spain), profusely used in the Granada's architectural and sculptural heritage, and with well-known problems connected with salt weathering [49]. The saline solutions were poured into cylindrical (12 cm diameter, 10 cm high) glass beakers where limestone slabs with dimension $3 \times 3 \times 25$ cm were vertically placed. The surface of the saline solution (without-control- and with added FC) was covered with melted paraffin wax to avoid excessive evaporation and undesired creeping and to promote solution capillary flow through the stone

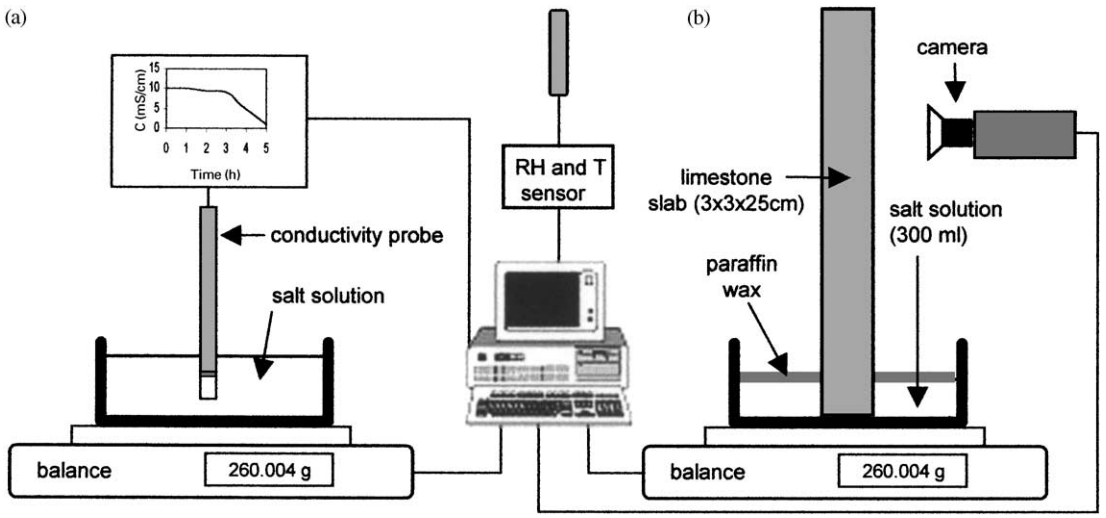

Fig. 1. Experimental set-up for sodium chloride crystallization: (a) open beakers, and (b) crystallization within porous stones (flow-through tests).

pore system (for details on the experimental setup see [27,28]). Once the solution percolated thought the porous stone, it eventually reached the stone surface where evaporation and crystallization of the salt began. This process is also known as the "wick effect" [50]. The salt efflorescence growth as well as the eventual superficial damage to the limestone were photographically recorded using time-lapse methods. The solution evaporation rate was measured by continuous weighing of the stone–solution–beaker system using a balance. NaCl crystals were collected after crystallization experiments, mounted in Al sample holders and examined by powder X-ray diffraction (XRD) with no prior treatment (i.e., no grinding) in order to infer their growth morphology. A Philips PW-1710 X-ray diffractometer with automatic slit, Cu K_α radiation ($\lambda = 1.5405$ Å), 3–90° 2θ explored area, with steps of 0.028° 2θ and 0.01° $2\theta\,s^{-1}$ goniometer speed, was used. Bragg peak intensities were compared with control powdered (i.e., disoriented) NaCl crystals, in order to determine which crystal faces were preferentially developed in the presence of the FC. Crystal morphologies and size distribution were further studies by means of optical microcopy (Jenapol-V) and scanning electron microscopy (SEM, Zeiss DMS 950). EDX microanalysis (coupled to the SEM) as well as cathodoluminescence (CTL) microscopy analysis [51] were used to qualitatively ascertain if irreversible adsorption of FC onto the growing NaCl crystals occurred. In addition, quantitative atomic absorption (AA, Perkin-Elmer 5100) spectrometric analyses (Fe content) were performed. Once NaCl crystallization in the presence of FC took place, the crystals were extracted from the mother solution, washed with pure saturated NaCl solution, filtered and dried before CTL, EDX and AA analyses.

The induction time for the onset of NaCl crystallization in the presence and absence of FC was evaluated by conductivity measurements (Crisom Instruments, mod. 525 with Pt electrode cell and automatic T correction) using equal-radius beakers filled with saline solution and let to freely evaporate (Fig. 1). To prevent formation of salts at the solution–air–glass interface and their eventual creeping, a thin layer of silicon grease (Apiezon) was spread over the internal glass surface. On-line weight-loss measurements were carried out simultaneously to the conductivity measurements in order to determine the supersaturation reached when crystallization started and to evaluate possible changes in solution evaporation rate due to the presence of the additives. Possible changes in solution surface tension in the presence of additives were evaluated using the pullout ring method (DyNouy Tensiometer, model CSC No. 70535) as described in Ref. [25]. Changes in the saline solution–calcite contact angle due to the presence of additives were determined by placing solution drops (using a syringe) onto large "Iceland Spar" calcite crystals cut along the $\{1\,0\,\bar{1}\,1\}$ cleavage planes and placed on an optical bench coupled to an on-line video recording system as in Ref. [25].

Small stone pieces ($\sim 3\,mm^3$) and NaCl efflorescence were collected from the stone slabs submitted to salt crystallization test and gold-coated prior to SEM analysis. NaCl crystals distribution within the stone pore system was inferred by means of mercury intrusion porosimetry (MIP, Micromeritics Autoscan 6500). Stone samples ($\sim 2\,cm^3$) were collected before and after salt crystallization tests and dried overnight in an oven (110°C) prior to MIP analysis.

3. Results and discussion

3.1. Critical supersaturation and crystallization

The addition of FC in the working concentrations neither changed NaCl solubility, nor modified the saline solution evaporation rate (open beakers): i.e., the evaporation rate of NaCl solutions was $1.95 \times 10^{-6}\,g\,s^{-1}\,cm^{-2}$ regardless of the FC presence. However, significant changes in both the induction time and the critical supersaturation (i.e., maximum relative supersaturation reached before the onset of crystallization) were observed (Fig. 2). The critical relative supersaturation, $\sigma(\sigma = 100(C - C_0)/C_0$, being C and C_0 the actual and the saturation concentrations, respectively) for pure NaCl solution was 1.3%, while the presence of 2.48×10^{-3} M $[Fe(CN)_6]^{4-}$ increased σ

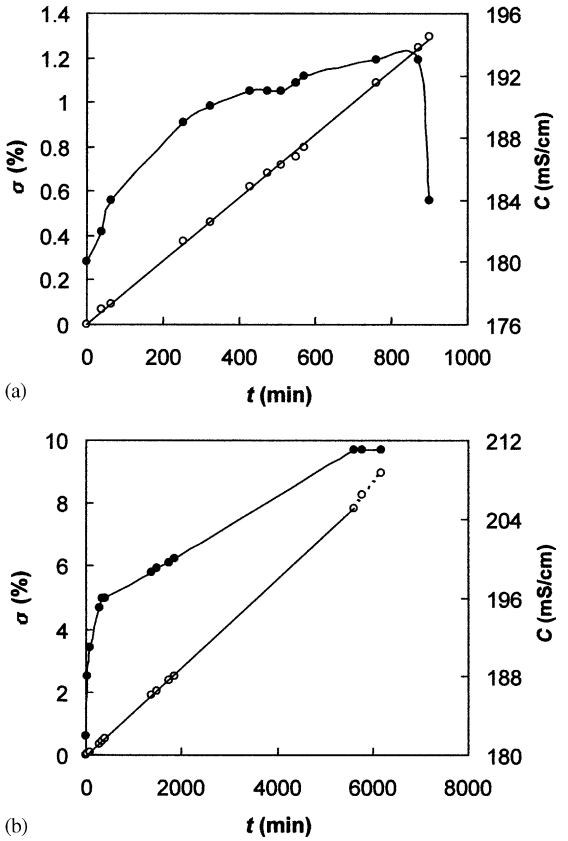

Fig. 2. Supersaturation (σ; full dots) and conductivity (C; open dots) evolution vs. time, following evaporation of a NaCl saturated solution (a) and a NaCl saturated solution with added 2.85×10^{-3} M $[Fe(CN)_6]^{4-}$ (b). Dotted line indicates NaCl crystals are present.

up to 8%. Conductivity measurements were accurate to determine the onset of NaCl crystallization in the absence of additive (i.e., see the conductivity sharp drop in Fig. 2a). However, no significant conductivity change was detected following the onset of NaCl crystallization (visually detected) in the presence of additives (Fig. 2b). This suggests that a significant concentration of additive was still available to prevent further NaCl nucleation, allowing a very high supersaturation to be sustained. The observed σ results match those of Van Damme-Van Wheele [43] and Glasner and Zidon [44] who found that the increase in critical relative supersaturation for NaCl nucleation vs. $[Fe(CN)_6]^{4-}$ concentration followed the power law $[\sigma] = Ax^B$, where $[\sigma]$ is the supersaturation in molar concentration, x is $[Fe(CN)_6]^{4-}$ concentration, and A and B are constants ($A = 3.47-3.76$, and $B = 0.23-0.24$). The results above described suggest that nucleation inhibition, which depends on additive concentration, is the ruling mechanism of additive–NaCl interaction. Irreversible additive adsorption onto a growing face according to the Cabrera and Vermilyea's model [6] does not seem to play a significant role (as will be discussed later), although limited irreversible adsorption occurred. The latter is demonstrated by AA results showing 57 ppm of Fe in the NaCl crystals grown in the presence of the maximum FC concentration (2.85×10^{-3} M) while only 1 ppm was present in the control NaCl crystals. The former Fe concentration is $\sim$10 wt% of that of the added FC. This low adsorption value is consistent with both CTL analyses showing no detectable increase in cathodoluminescence intensity in the crystals grown in the presence of the additive, and EDX analyses which failed to detect any Fe in the latter crystals. The possible role of limited reversible additive adsorption according to the Lacmann and Stranski's model [52] will be discussed later.

3.2. Solution properties and evaporation rate: efflorescence vs. subflorescence growth

The evaporation rate of the solution with additives percolating through the stone was much higher than that of pure NaCl solution (Fig. 3). Two phenomena can be accounted for this effect:

(i) A reduction of the solution surface tension γ could lead to a reduction of the capillary pressure P in a pore of radius r, inducing a faster evaporation (i.e., same action as that of surfactants in the crack-free drying of green clay bodies [53]) since the Laplace's equation states that

$$\Delta P = -\frac{2\gamma}{r}. \quad (1)$$

Conversely, a reduction in solution–stone contact angle θ due to FC adsorption onto the stone porewalls (calcite) could lead to faster capillary supply toward the evaporation front, thus promoting evaporation. The relation between the rate of capillary rise in such a system is described by

Washburn's equation [54]

$$h^2 = \frac{tr\cos\theta\gamma}{2\eta}, \quad (2)$$

where t is the time it takes for the liquid to rise a distance of h centimeters, and η is the viscosity of the liquid. No significant changes in both the saline solution surface tension and the calcite–solution contact angle were detected upon addition of FC (Table 1). On the one hand, these results reflect that FC adsorption onto the stone pore walls was negligible (i.e., almost all the additive was in solution following flow through the stone pore system). On the other hand, the observed evaporation rates do not seem to be due to changes in the solution physical properties.

(ii) the formation of a significant amount of porous efflorescence on the stone surface in the presence of FC (right from the start of the crystallization experiment) leads to an important increase of the surface area of the evaporation front, strongly contributing to the exponential increase of the evaporation rate observed in Fig. 3; an increase which is somewhat proportional to the FC concentration. Fig. 4 shows the efflorescence formed on the stone surface.

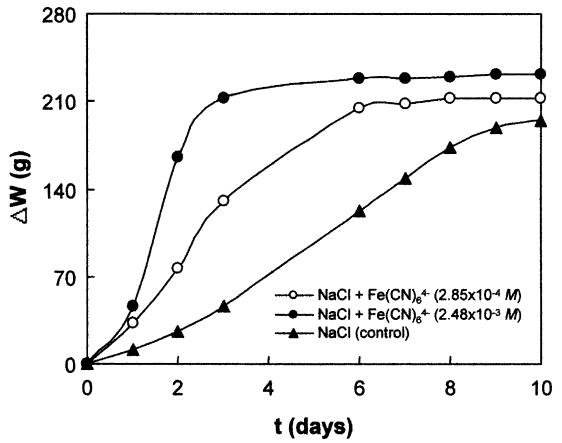

Fig. 3. Weight loss (due to evaporation of the saline solution flowing through the porous stone) vs. time for the solutions without (control) and with additive.

Efflorescence acts as a saturated porous network with a very high surface area, which notably increases the evaporation rate. This effect is similar to that caused by "rampant" or "creeping" salts [55]. It should be noted that the former effect was also observed (although in a limited way) in the very late stages of solution evaporation in the open beakers, when salts crept over the beakers walls. The increase in evaporation rate ultimately led to an even greater critical supersaturation (see below).

All in all, crystallization of NaCl in the presence of FC results in the massive formation of efflorescence on the stone surface, while a lesser amount of efflorescence is observed in the controls. It has been experimentally demonstrated that NaCl crystals tend to grow within porous stone thereby resulting in stone disintegration by crystallization pressure build up [28]. The situation is exacerbated when high evaporation rates (due to low relative humidity or high T) exist, since a faster evaporation promotes a higher supersaturation [28,56–58]. The crystallization pressure P exerted by a salt in a confined space (i.e., a pore) is given by Correns's equation [31]

$$P = \frac{RT}{V_m}\ln\frac{C}{C_0}, \quad (3)$$

where R is the gas constant, T is the temperature, V_m is the molar volume of the solid phase and C/C_0 is the supersaturation. It follows from

Table 1
NaCl aqueous solution (1.22 M) contact angle[a], θ (in degrees), and surface tension, γ (in mN/m)[b], in the presence of $[Fe(CN)_6]^{4-}$

Sample	θ	γ
DI water	45±18 (8)	71.97±0.05 (3)
NaCl solution	29±1 (4)	78.00±0.16 (4)
NaCl solution + 0.01 M $[Fe(CN)_6]^{4-}$	47±15 (6)	78.02±0.16 (4)
NaCl solution + 0.05 M $[Fe(CN)_6]^{4-}$	30±6 (6)	78.37±0.19 (4)

[a] Measured on freshly cleaved Iceland spar calcite (1 0 $\bar{1}$ 1) crystal faces.
[b] Average values, standard deviations (and number of measurements) are presented.

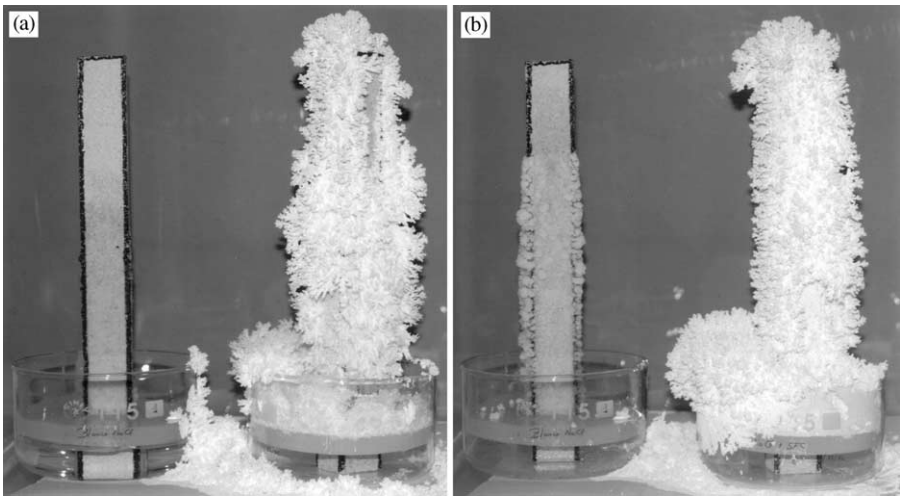

Fig. 4. Photographs of porous calcareous stone slabs following 48 h (a) and 7 days (b) NaCl saturated solution flow-through and evaporation/crystallization, in the case of a pure solution (left stone slab) and a solution with 2.85×10^{-3} M $[Fe(CN)_6]^{4-}$ (right stone slab). Note that in the control sample most of the solution was still in the beaker following 48 h, while a very small amount of solution remained in the sample with the additive (a). The solution in the control was completely evaporated after 1 week when limited efflorescene growth was observed (b).

Eq. (3) that the higher the supersaturation, the higher the crystallization pressure will be. In the present case, some NaCl crystals in the control run crystallize within the stone pores (as subflorescence), generating enough crystallization pressure to induce granular disintegration. This type of damage occurred at the stone slab upper edges and corners in the control run (i.e., areas of faster evaporation). MIP results show that in this case a small volume of pores are filled with salt (Fig. 5). According to Lewin's model [59], salt crystallization as subflorescence occurs because the evaporation at the stone surface is faster than the solution replenishment from inside the porous body, resulting in both the retraction of the evaporation front deep into the stone and the crystallization of the salt within a confined space (a pore) where crystallization pressure is built up. However, in the presence of FC negligible subflorescence occurred since almost all crystallization took place on the stone surface as efflorescence. No damage was detected in this latter case, although the higher supersaturation reached in the presence of FC would, theoretically, result in higher crystallization pressure. However, for damage to occur, crystallization should have taken place in a confined space.

3.3. The effect of $[Fe(CN)_6]^{4-}$ ions on NaCl growth morphology

Fig. 6 compares XRD patterns of NaCl crystals formed in the absence and in the presence of FC. Both sodium and potassium ferrocyanide induce similar and significant habit modifications in NaCl crystals, even at the lowest concentration ($\sim 10^{-4}$ M $[Fe(CN)_6]^{4-}$) in both the stone efflorescence (Fig. 6b) and in the open beakers (Fig. 6c). In particular, the most common cube {1 0 0} forms in the control sample are hindered in the presence of FC as inferred from the significant intensity reduction of the 200 Bragg peak. Conversely, the strong intensity increase of the 220 Bragg peak evidences the significant development of the dodecahedron {1 1 0} faces. The octahedron {1 1 1} and tetrahexahedron {2 1 0} forms are also preferentially developed in the presence of FC, as shown by a moderate increase in the intensities of 111 and 222, as well as 420, Bragg peak. However, the latter forms are less abundant than {1 1 0}.

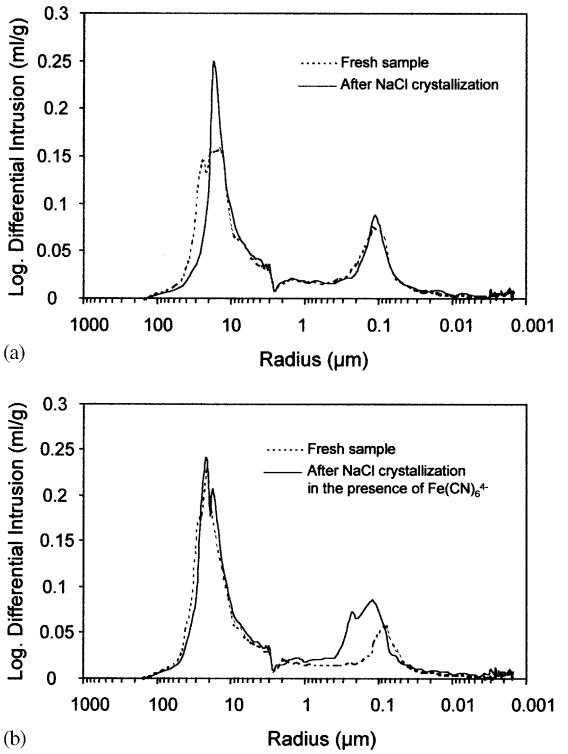

Fig. 5. Mercury intrusion porosimetry plots showing pore size distribution (i.e., $\log(dv/dr)$ vs. r, where v is the intruded volume and r the pore radius), for a control sample (a) and a sample submitted to NaCl crystallization in the presence of 2.6×10^{-3} M $[Fe(CN)_6]^{4-}$ (b). In both cases it is shown the curve corresponding to the stone before any crystallization occurred (dotted line) and after crystallization (solid line).

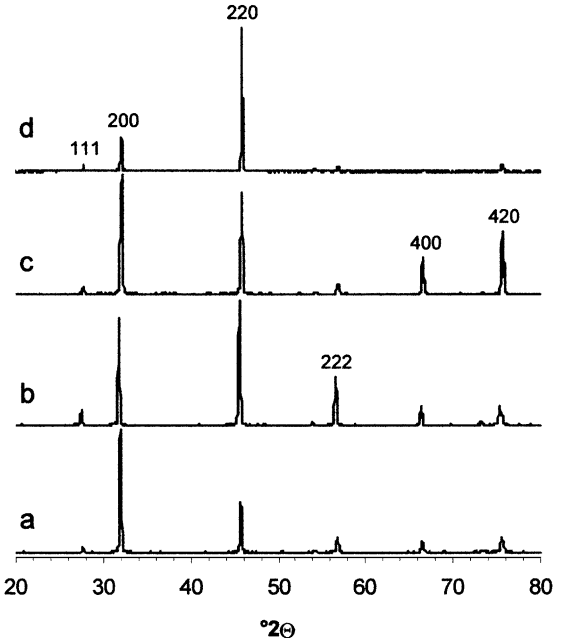

Fig. 6. Results of the XRD analysis of: (a) NaCl crystals (control); (b) NaCl crystals formed following crystallization in the porous stone in the presence of 2.4×10^{-4} M $[Fe(CN)_6]^{4-}$; (c) NaCl crystals formed following solution evaporation in an open beaker in the presence of 2.48×10^{-3} M $[Fe(CN)_6]^{4-}$; (d) NaCl crystals formed following partial solution evaporation in an open beaker in the presence of 2.48×10^{-3} M $(Fe(CN)_6)^{3-}$: in this case the XRD analysis was performed on wet samples (i.e., NaCl crystals surrounded by solution).

Strikingly, wet samples (still with solution within the NaCl crystals network) collected both from the stone efflorescence and from the "creeping salts" formed in the crystallization dishes show the largest increase in 220 Bragg peak intensity (Fig. 6d).

SEM images are consistent with the XRD results, and offer a more detailed picture of the changes in NaCl crystals morphology induced by FC. Fig. 7a shows the most common {1 0 0} form in the control sample. The increased evaporation rate in the porous stone (control run with no FC) led to a higher supersaturation and the formation of NaCl hollow-faced {1 0 0} forms (Fig. 7b), while some {1 1 1} forms were also observed. In the presence of FC skeletal and dendritic growth was observed (Fig. 7c–f). In the open beakers, NaCl dendrites tended to grow with their growth axis parallel to the ⟨1 1 1⟩ direction, as evidenced by the development of branches at 120° with well-developed {1 1 0} faces (Fig. 7c). Stone efflorescence grown in the presence of FC included skeletal crystals with fractal geometry (Fig. 7d), branched dendrites growing along ⟨1 1 1⟩ direction with poorly developed {1 1 0} faces (Fig. 7e), and skeletal hopper crystals with {1 1 0} faces forming a spiral-like structure (Fig. 7f). It seems that dendrites growing along ⟨1 1 1⟩ and limited by well-developed {1 1 0} faces develop at a lower supersaturation as inferred by their massive presence in the wet salt samples (XRD results), while the amount of {1 1 0} faces is relatively reduced when crystallization was completed (i.e., full drying). It should be noted that during the last

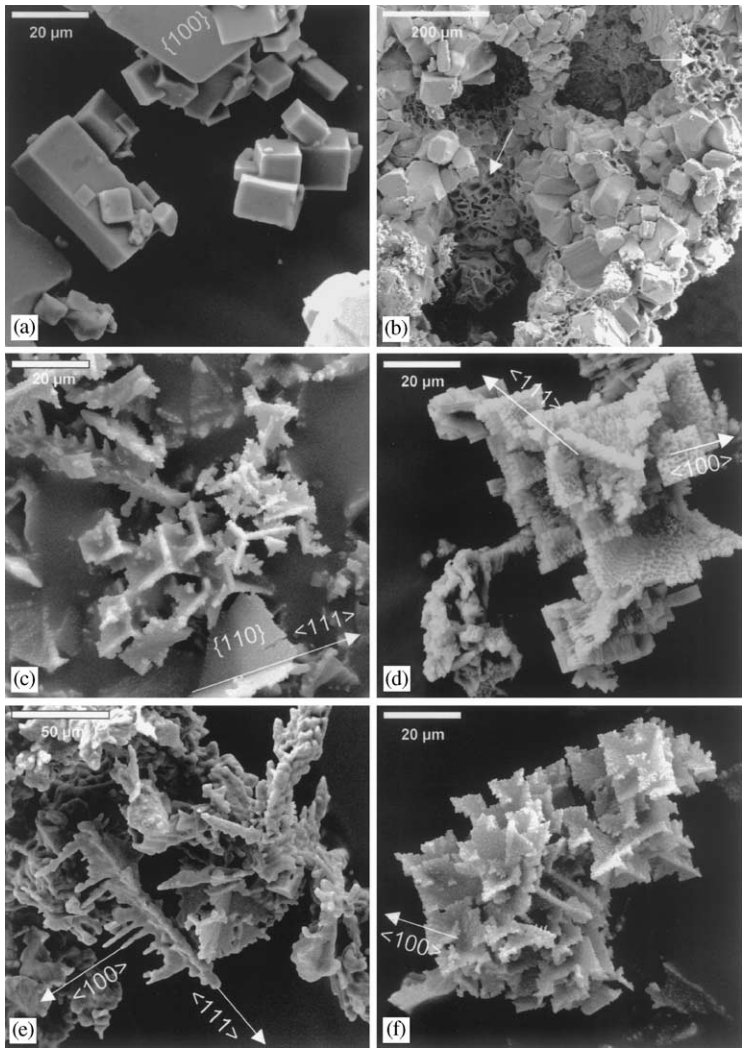

Fig. 7. SEM photomicrographs showing NaCl crystals: (a) {1 0 0} forms in the control solution; (b) hollow-faced halite crystals (arrows) formed on the stone surface (control run); (c) elongated NaCl crystals with well-developed {1 1 0} faces formed in the presence of $[Fe(CN)_6]^{4-}$; (d) skeletal NaCl crystals formed in the presence of ferrocyanide on the stone surface; (e) dendrites formed on the stone surface in the presence of $[Fe(CN)_6]^{4-}$ which are elongated along ⟨1 1 1⟩ and side-branched along ⟨1 0 0⟩; (f) skeletal crystals formed in the stone efflorescence in the presence of $[Fe(CN)_6]^{4-}$ with well-developed {1 1 0} faces and forming spirals-like structures growing along ⟨1 0 0⟩.

stages of drying formation of efflorescence and salt creeping occurred both in the stones and (to a lesser extent) in the open beakers, which may imply an increase in the evaporation rate and higher supersaturation. This seems to induce the formation of dendrites with poorly developed {1 1 0} faces resulting in the relative decrease in 220 Bragg peak intensity observed in the dry samples if compared with the wet ones.

Two main effects, resulting in an increased supersaturation, can account for the changes in NaCl crystal morphology from cube to octahedron and to hopper crystals [54–56] when crystallization occurs in the porous stone in the absence of FC: (i) first, because of the increase in supersaturation resulting from the higher evaporation rate of the solution in the porous stone (if compared with the open beakers) due to its large

specific surface area of $\sim 4\,m^2\,g^{-1}$ (determined by MIP); and (ii) second, because of the higher supersaturation a solution can sustain in a porous media (with pores with $r < 1\,\mu m$) before crystallization starts due to the Laplace effect of curvature of the solution in a capillary or a pore [60]. Once the solution reaches a larger pore, or the stone surface, the Laplace's effect of curvature no longer applies, and the highly supersaturated solution reaching the evaporation front rapidly crystallizes.

The former effects add to the inhibiting action of the additives. In the late 1950s and early 1960s, Kern and co-workers [40,41,56–58] found that alkaline halide crystals (e.g., NaCl, KCl, KBr, KI) tend to modify their growth morphologies either due to a change in evaporation rate (or solution T) resulting in a high supersaturation, or to the presence of additives. A high supersaturation decreased the relative amount of solvent (i.e., water molecules) in the solution and favored the growth of octahedron and dodecahedron faces [57,58,61]. The additives were observed to play a dual role: they delayed the incorporation of solute ions into any face of a growing crystal, thereby increasing the solution supersaturation, and/or they changed the faces relative growth rate following their adsorption. Boistelle et al. [40] found that iron cyanides (both ferri- and, particularly, ferrocyanides) were important NaCl habit modifiers. They observed that ferricyanides changed NaCl growth form from $\{1\,0\,0\} \rightarrow \{1\,1\,1\} \rightarrow \{1\,1\,0\}$ for increasing additive concentration. However, they were not able to determine this same sequence (i.e., morphodrome) for ferrocyanides. Instead, they observed the transition from $\{1\,0\,0\}$ to dendritic growth, with an intermediate stage where $\{1\,0\,0\}$ faces developed many small cubes growing along [1 0 0] directions (i.e., skeletal crystals). Van Damme-Van Weele [43] found that ferricyanides were less able than ferrocyanides to induce high supersaturations, the latter always promoting NaCl dendritic growth. We have observed that the supersaturation reached before NaCl crystallization in the presence of ferrocyanides is relatively high (Fig. 2b), and results in a change in growth morphology from $\{1\,0\,0\}$ to $\{1\,1\,0\}$, particularly in the open crystallization dishes where a somewhat limited supersaturation is reached, while more significant morphology changes are observed in the porous stone crystallization tests where dendritic growth is favored. NaCl dendrites (and dendrites in general) are reported to develop at very high supersaturation [62] as will be discussed below.

3.4. NaCl dendritic growth

The formation of stable spatial patterns such as dendrites is a common feature in nonlinear, nonequilibrium systems [63]. Diffusion-limited growth of a crystal in a supersaturated medium commonly results in dendritic patterns (e.g., ice-crystal dendrites [64]). Diffusion limits the rate at which a crystal can grow, often greatly affecting the growth shape in the process. An important mechanism by which this happens is the Mullins–Sekerka instability [65], which causes simple growing crystals to assume complex shapes. This instability emerges when a roughness or a bump emerges on flat surface growing in a supersaturated medium. The bump tends to grow faster than the surrounding surface since it induces a higher concentration gradient that promotes diffusion towards the bump tip; thereby the instability is self-amplified. The net result is that the flat growth is unstable, and a crystal will tend to grow into more complex shapes: e.g., dendrites. In the case of NaCl crystals the corners and edges stick out most; therefore these grow the fastest, robbing ions from the centers of the faces, which then grown much more slowly. This results in hopper crystals development when growth takes place along $\langle 1\,1\,1 \rangle$ (i.e., edges), or in dendritic growth along $\langle 1\,1\,0 \rangle$ (i.e., corners) with side-branching along $\langle 1\,0\,0 \rangle$ at higher supersaturation, as observed here. If the dendrite tip grow velocity is above a certain threshold, the $\{1\,1\,0\}$ faces parallel to the dendrite $\langle 1\,1\,1 \rangle$ growth axis (i.e., their zone axis) are not developed fast enough, and side-branches along $\langle 1\,0\,0 \rangle$ directions are formed as observed in Fig. 7e.

Morphology changes connected with increasing supersaturation are primarily due to a change in the crystal faces growth mechanism [66]: from screw dislocation driven, to two-dimensional

nucleation, towards dendritic growth through rough surface continuous adhesion at the highest supersaturation. These growth-mechanism changes, which ultimately dictate which face will grow fastest, are consistent with the existence of different face-types according to Hartman and Perdoc's PBC model [67]: i.e., screw or two-dimensional growth rules in F faces, while rough-surface adhesion is promoted on S and, particularly, on K faces (i.e., {1 0 0}, {1 1 0} and {1 1 1} NaCl faces, respectively [68]). Therefore, the last ones will be less developed at high supersaturation, explaining for instance why preferential NaCl dendritic growth with poor development of {1 1 0} faces takes place along ⟨1 1 1⟩ in the stone efflorescence (i.e., fastest grow along ⟨1 1 1⟩ directions). Nevertheless, a limited amount of NaCl crystals with {1 1 1} forms are observed in the stone efflorescence grown in the absence of additive (SEM results), and in the crystallization dishes when NaCl growth occurs in the presence of FC (XRD results). In this particular case, the development of {1 1 1} faces is explained considering that: (a) water is a special case among polar solvents because it can interact strongly with halide ions by the formation of hydrogen bonds [69], and (b) at a relatively high supersaturation (not sufficiently high for hopper crystals or dendrites development) the relative concentration of solvent (i.e. water) molecules is reduced, and {1 1 1} faces which are composed of alternating layers of Na^+ and Cl^- ions (i.e., strongly solvated) will grow slower than less-strongly solvated {1 0 0} faces [57,58], as the removal of the adsorbed water dipoles becomes the rate determining step. As the electrostatic field strength normal to the cube face is much lower, the adsorption here is much weaker. Hence, it is possible that the growth of {1 1 1} is slowed down even below $1/3^{1/2}$ times the growth rate of the cube [70]. However, above a certain supersaturation threshold rough interface growth is promoted [66] resulting in fastest growth along ⟨1 1 0⟩ (i.e. hopper crystals) and ⟨1 1 1⟩ (i.e. dendrites).

3.5. The ultimate role of $[Fe(CN)_6]^{4-}$ ions on NaCl growth on porous stone

Regarding the ultimate inhibiting mechanism of FC on NaCl nucleation and growth, it should be mentioned that contrary to what was believed in the 1960s (see [43]), the effects of FC as crystallization inhibitors for NaCl are mainly constrained to the nucleation stage: i.e., they seem to be very effective nucleation inhibitors with a minor role as growth inhibitors. $[Fe(CN)_6]^{4-}$ ions have a strong tendency to solvate in aqueous solution. Therefore, they can both reduce the concentration of available solvent (i.e., water) in the system, thereby increasing the relative supersaturation, and by adsorbing Na^+ ions they can interfere ion transport towards more or less developed NaCl clusters with dimensions below the critical radius [71]. This way, $[Fe(CN)_6]^{4-}$ ions act as Na^+ scavengers. On the other hand, $[Fe(CN)_6]^{4-}$ ions do not seem to be irreversibly adsorbed onto growing faces; at least they do so in no significant proportion as indicated by the low Fe content in NaCl crystals grown in the presence of FC (AA analysis). This is also consistent with the poor development of {1 1 1} forms in the efflorescence where dendrites grow fastest along ⟨1 1 1⟩. The existence of a large number of kinks and steps on sodium chloride K (i.e., {1 1 1}) and, to a lesser extent, S (i.e., {1 1 0} and {2 1 0}) faces, would made them the most adequate for additive molecules adsorption. It should be expected that a strongly negative anion such as ferrocyanide would be preferentially adsorbed onto {1 1 1} faces where alternating close-packed layers of Na^+ and Cl^- exist (i.e., in a similar manner as the effect of urea inducing changes from cube to octahedron on NaCl morphology). The ferrocyanide ion has an octahedral configuration with six $(CN)^-$ ions (with $\frac{1}{2}$ negative charge) at the corners [72]. Therefore, it could be adsorbed through its octahedral faces on NaCl {1 1 1} faces by electrostatic bonding with the Na^+. However, this does not seem to be the case here, an observation consistent with the very limited adsorption of FC onto growing NaCl crystals and almost absence of {1 1 1} forms. Furthermore, the ~15% misfit between the $K_4[Fe(CN)_6]\cdot 3H_2O$ and the NaCl lattice (the misfit is even greater for $Na_4Fe(CN)_6\cdot 10H_2O$) precludes the formation of a monolayer cover on the NaCl crystals [44]. There exist, however, the possibility of reversible adsorption onto a given flat face, according to the model presented by

Lacmann and Stranski [52], but this model predicts the development of F faces (i.e., NaCl {1 0 0} faces) which is not consistent with our XRD and SEM results. Alternatively, Glasner and Zidon [44] proposed that sodium chloride heterogeneous nucleation on FC due to the good structural and size matching between the $[Fe(CN)_6]^{4-}$ ions and the hexaclorosodium $[NaCl_6]^{5-}$ configuration in the NaCl lattice could explain the reported effect of this additive. The inconsistency between this aided heterogeneous nucleation model and the observed high supersaturation was apparently solved by claiming that many crystallite particles below the critical radius would be present and would not crystallize spontaneously. However, this model is not consistent with our conductivity results (Fig. 2b) showing a continuous conductivity rise as the supersaturation increases till an asymptotic value is reached when NaCl crystals are visually detected. If heterogeneous nucleation on $[Fe(CN)_6]^{4-}$ ions would have taken place as soon as evaporation reached the saturation point, as postulated in Ref. [44], the asymptotic value should have been reached much earlier.

All results suggest that FC are very powerful nucleation suppressors. In the stone, this effect promotes efflorescence growth mostly by inhibiting NaCl nucleation in the stone pores. Efflorescence, which acts as a saturated porous (fractal) media, contributes to the migration of the evaporation front towards the outer efflorescence surface inducing the growth of more efflorescence further away. Efflorescence progresses in a periodic self-similar way as first described for "creeping salts" [54]. All in all, the system acts as a solution pump, extracting the saline solution from the reservoir through the porous stone towards the evaporation front, and resulting in a constantly increased evaporation rate. This contributes to the further formation of efflorescence that does not harm the stone when crystallization takes place.

4. Conclusions

The addition of ferrocianides to NaCl solutions induces significant changes both on the dynamics and kinetics of solution flow-through and evaporation within a porous material, as well as on the critical supersaturation and crystallization pattern of NaCl.

FC are demonstrated to be effective against salt damage as they promote NaCl efflorescence growth as opposed to subflorescence growth in porous stones. This appears to be largely due to the demonstrated inhibiting role of the additive on NaCl nucleation which prevent this salt from crystallizing within the pores of the stone, inducing its crystallization where a very high supersaturation occurs, i.e., at the stone surface, where evaporation is maximum.

The rapid development of efflorescence on the stone surface in the presence of FC contributes to the increase in the evaporation rate by creating a porous, fractal media with a high surface area (i.e., self-feeding mechanism). This together with the inhibiting effect of $[Fe(CN)_6]^{4-}$ ions on NaCl nucleation, results in the development of skeletal crystals with {1 1 0} faces and dendrites growing along $\langle 1\,1\,1 \rangle$, as opposed to the most common {1 0 0} form.

It is concluded that the extremely high supersaturation reached in the presence of the additive before NaCl crystallization on the stone surface changes the growth mechanism of NaCl faces from screw or two-dimensional growth, toward surface adhesion on rough surfaces (i.e., S and, specially, K faces).

Finally, the addition of FC in very low concentration (10^{-4}–10^{-3} M) to ornamental stones affected by NaCl crystallization, may provide a new way to minimize salt damage and aid in the desalination of salt contaminated stone. From a practical point of view, the application of poultices impregnated with ferrocyanide aqueous solution may provide an important new procedure to desalinate salt-laden stones. However, additional laboratory and field-testing is needed before such a method could be applied.

Acknowledgements

This work has been supported by grant No. MAT2000-1457 from the Spanish government, the

Research Group NMR 0179 of the Junta de Andalucia (Spain), and the Getty Conservation Institute through the Salt Damage project. We also thank the Centro de Instrumentación Científica of the universidad de Granada for technical assistance during SEM analyses. We are grateful to D. Carson who performed surface tension and contact angle measurements.

References

[1] H.E. Buckley, Crystal Growth, Chapman & Hall, London, 1952.
[2] J.W. Mullin, Crystallization, 3rd Edition, Butterworth, London, 1992.
[3] J.B.L. Romé de L'Isle, Cristallographie, Iimpremiere du Monsieur, Paris, 1783.
[4] K. Sangwal, Prog. Crystal Growth Charact. 32 (1996) 3.
[5] M. Lahav, L. Leiserowitz, J. Phys. D 28 (1993) B22.
[6] N. Cabrera, D.A. Vermilyea, in: R.H. Dorenus, B.W. Robert, D. Turnbull (Eds.), Growth and Perfection of Crystals, Wiley, New York, 1958, p. 393.
[7] A.A. Chernov, Modern Crystallography III: Crystal Growth, Springer, Berlin, 1984.
[8] K. Sangwal, J. Crystal Growth 128 (1993) 1236.
[9] K. Sangwal, Prog. Crystal Growth Charact. 38 (1998) 163.
[10] H. Füredi-Milhofer, S. Sarig, Prog. Crystal Growth Charact. 32 (1996) 45.
[11] S. Veintemillas-Verdaguer, Prog. Crystal Growth Charact. 32 (1996) 75.
[12] P.H. Ralston, Mater. Prot. Perform. 11 (1972) 6.
[13] G.M. van Rosmalen, Chem. Eng. Commun. 20 (1983) 209.
[14] P. Gu, V.S. Ramachandran, J.J. Beaudoin, E. Quinn, Adv. Cem. Bas. Mater. 2 (1995) 182.
[15] F.H. Butt, F. Rahman, U. Baduruthamal, Desalination 103 (1995) 189.
[16] P.G. Klepetsanis, P.G. Koutsoukos, J. Crystal Growth 193 (1998) 156.
[17] S. He, A.T. Kan, M.B. Tomson, Appl. Geochem. 14 (1999) 17.
[18] C. Garcia, G. Courbin, F. Ropital, C. Fiaud, Electrochim. Acta 46 (2001) 973.
[19] M.E. Tadros, I. Mayes, J. Colloid Interface Sci. 72 (1979) 245.
[20] D. Bosbach, M.F. Hochella, Chem. Geol. 132 (1996) 227.
[21] E. Badens, S. Veesler, R. Boistelle, J. Crystal Growth 198/199 (1999) 704.
[22] D.H. Oza, R.K. Safre, Indian J. Tech. 14 (1976) 435.
[23] A. Zafiropoulou, E. Dalas, J. Crystal Growth 219 (2000) 477.
[24] S.N. Black, L.A. Bromley, D. Cottier, R. Davey, B. Dobbs, J.E. Rout, J. Chem. Soc. Faraday Trans. 87 (1991) 3409.
[25] C. Rodriguez-Navarro, E. Doehne, E. Sebastian, Langmuir 16 (2000) 947.
[26] I.E. Evans, Rev. Géomorphol. Dyn. 19 (1970) 155.
[27] C. Rodriguez-Navarro, E. Doehne, Am. Lab. 31 (1999) 28.
[28] C. Rodriguez-Navarro, E. Doehne, Earth Surf. Process. Landforms 24 (1999) 191.
[29] D. Benavente, M.A. Garcia del Cura, R. Fort, S. Ordonez, J. Crystal Growth 204 (1999) 168.
[30] G. Scherrer, Cem. Concr. Res. 29 (1999) 1347.
[31] C.W. Correns, Discuss. Faraday Soc. 5 (1949) 267.
[32] E.M. Winkler, P.C. Singer, Geo. Soc. Am. Bull. 83 (1972) 3509.
[33] La Iglesia, V.González, V. López-Acevedo, C. Viedma, J. Crystal Growth 1777 (1997) 111.
[34] A.S. Goudie, H. Viles, Salt Weathering Hazards, Wiley, Chichester, 1997.
[35] K. Zehnder, A. Arnold, J. Crystal Growth 97 (1989) 513.
[36] V. Lopez-Acevedo, C. Viedma, V. Gonzalez, A. La Iglesia, J. Crystal Growth 182 (1997) 103.
[37] C. Selwitz, E. Doehne, J. Cultural Heritage (2002), in press.
[38] R.W. Chapman, Am. J. Sci. 280 (1980) 116.
[39] M.M. Prebble, Nature 216 (1967) 1194.
[40] R. Boistelle, R. Kern, R. Weiss, C. R. Acad. Sci. 254 (1962) 1829.
[41] M. Bienfait, R. Boistelle, R. Kern, C. R. Acad. Sci. 256 (1963) 2189.
[42] C.T. Roland, P.H. Ralston, Canadian Patent No. 765.644, 1963.
[43] I.M.A. van Damme-van Weele, Influence of additives on the Growth and Dissolution of Sodium Chloride Crystals, Ph.D. Thesis, Technical University Twente, Enschede, Netherlands, 1965;
I.M.A. van Damme-van Weele, in: R. Kern (Ed.), Adsorption et Croissance Cristalline, Coll, CNRS 152 (1965) 433.
[44] A. Glasner, M. Zidon, J. Crystal Growth 21 (1974) 294.
[45] H.H. Emons, Freiberg. Forschungsh. A 600 (1979) 73.
[46] Transportanion Research Board, Special Report 235, Highway Deicing: Comparing Salt and Calcium Magnesium Acetate, National Research Council, Washington, DC, 1991.
[47] Salt Institute, Deicing Salt and Our Environment. Salt Institute, Alexandria VA, 1996.
[48] T.B. Hansen, L.H. Skibsted, H.J. Andersen, Meat Sci. 43 (1996) 135.
[49] C. Rodriguez-Navarro, Causas y Mecanismos de Alteración de los Materiales Calcáreos de las Catedrales de Granada y Jaén, Ph.D. Thesis, Granada University, Granada, 1998.
[50] A.S. Goudie, Earth Surf. Process. Landforms 11 (1986) 275.
[51] B.G. Yacobi, D.B. Holt, Cathodoluminiscence Microscopy of Inorganic Solids, Plenum Press, New York, 1990.
[52] R. Lacmann, I.N. Stranski, in: R.H. Doremus, B.W. Roberts, D. Turbull (Eds.), Growth and Perfection of Crystals, Wiley, New York, 1958, p. 427.

[53] G.S. Scherer, J. Am. Ceram. Soc. 73 (1990) 3.
[54] E.R. Washburn, J. Phys. Chem. 31 (1927) 12.
[55] E.W. Washburn, Am. Phys. Soc. 2nd Ser. 17 (1921) 374; T.H. Hazlehurst, H.C. Martin, L. Brewer, J. Phys. Chem. 40 (1936) 439.
[56] R. Kern, C. R. Acad. Sci. 234 (1952) 970.
[57] R. Kern, Bull. Soc. Franç. Minér. Crist. 76 (1953) 325, 365.
[58] R. Kern, C. R. Acad. Sci. 236 (1954) 830.
[59] S.Z. Lewin, in: S.M. Barkin (Ed.), Conservation of Historic Stone Buildings and Monuments. National Academy of Sciences, Washington DC, 1981, p. 120.
[60] D. Kashchiev, G.M. van Rosmalen, J. Colloid Interface Sci. 169 (1995) 214.
[61] M. Bienfait, R. Boistelle, R. Kern, In: R. Kern (Ed.), Adsorption et Croissance Cristalline, Coll. CNRS 152 (1965) 515.
[62] M. Hille, H. Rau, J. Schlipf, in: R.H. Dorenus, B.W. Robert, D. Turnbull (Eds.), Growth and Perfection of Crystals, Wiley, New York, 1958, p. 325.
[63] G. Nicolis, I. Prigogine, Self-Organization in Nonequilibrium Systems, Wiley, New York, 1977.
[64] K.G. Libbrecht, T. Crosby, M. Swanson, Phys. Rev. Lett. 81 (1998) 176.
[65] W.W. Mullins, R.F. Sekerka, J. Appl. Phys. 34 (1963) 323.
[66] I. Sunagawa, Bull. Míner. 104 (1981) 81.
[67] P. Hartman, W.C. Perdock, Acta Crystallogr. 8 (1955) 49, 521, 525.
[68] R. Kern, Bull. Soc. Franç. Minér. Crist. 78 (1955) 497.
[69] A. Millan, J. Crystal Growth 208 (2000) 592.
[70] P. Hartman, in: P. Hartman (Ed.), Crystal Growth: an Introduction, North-Holland, Amsterdam, 1973, p. 367.
[71] Y.J. Twu, C.W.S. Conover, Y.A. Yang, L.A. Bloomfield, Phys. Rev. B 42 (1990) 5306.
[72] J.E. Huhneey, E.A. Keiter, R.L. Keiter, Inorganic Chemistry: Principle of Structure and Reactivity, 3rd Edition, Harper-Collins, New York, 1983.